Determination of the Micelle Architecture of Polystyrene/Poly(4-vinylpyridine) Block Copolymers in Dilute Solution

Markus Antonietti* and Steffi Heinz

Max-Planck-Institut für Kolloid und Grenzflächenforschung, Kantstrasse 55, D-14513 Teltow-Seehof, Germany

Manfred Schmidt and Christine Rosenauer

Makromolekulare Chemie II der Universität Bayreuth, Universitätsstrasse 30, D-95440 Bayreuth, Germany

Received October 18, 1993; Revised Manuscript Received March 18, 1994®

ABSTRACT: Block copolymers consisting of polystyrene (PS) and poly(4-vinylpyridine) (4-PVP) with varying chain lengths are synthesized via anionic polymerization. When these block copolymers are dissolved in selective solvents (solvents for PS), well-defined micelles with respect to their size and size distribution are formed. These micelles are characterized by static and dynamic light scattering. The characterization reveals that the micelles exhibit spherical or prolate morphology with a size in the range $20 \leq r_H \leq 100$ nm. Size and shape depend only on the block molecular weights and the solvent used but exhibit no significant concentration dependence. In certain solvents, the observation of scattering peaks indicates the formation of intermicellar ordering on the scale of the wavelength of light. Viscometric experiments reveal that the block copolymer micelles are unstable under shear applied in common viscometer tubes and decompose to the primary block copolymers. The associated structure, however, is quickly recovered.

(I) Introduction

For several years it has been known that polymer micelles are formed when block copolymers are dissolved in solvents for one of the components only. These micelles are well-defined with respect to their size and size distribution (see, for instance, refs 1–8).

In this paper, we describe the micellar morphology in dilute solution of block copolymers consisting of polystyrene (PS) and poly(4-vinylpyridine) (4-PVP) with varying chain lengths.

The system styrene/4-vinylpyridine was chosen for several reasons. On the one hand, both polymers possess nearly the same index of refraction[9] with simplifies the evaluation of light scattering data. On the other hand, the solution properties of PS and 4-PVP are sufficiently different to allow micelle formation in nearly all solvents. In addition, these polymers can be made in high quality and in large amounts by anionic polymerization.

The micelles of these block copolymers are characterized by static and dynamic light scattering in various solvents. This combination allows for determination of the aggregation number, the micelle size, architecture, and polydispersity.

The comparison of all these data with theory yields a more detailed picture of block copolymer aggregation and morphology in dilute solution. In addition, the influence of the aggregation number on the stretching of the chains in a micellar morphology can be estimated.

(II) Experimental Section

(II.1) Polymer Synthesis. The PS/4-PVP block copolymers are synthesized by anionic polymerization following standard procedures.[10,11] All reactions take place within our all-glass vacuum line which has already been described in the literature.[12,13] *sec*-Butyllithium (12% solution in hexane; Aldrich) is used to initiate the polymerization which is performed at −55 °C in tetrahydropyran (THP). Styrene is freshly distilled over lithium aluminium hydride, degassed, and added to the initiator solution via the gas phase.[12,13] The reaction is kept at this temperature for 15 min. A small amount of this solution is taken for characterization of the polystyrene block. Afterward, the calculated amount of 4-vinylpyridine (twice distilled over calcium hydride) is also added via the gas phase. A marked change of the color from yellow to red occurs, indicating the blocking from styrene to 4-vinylpyridine. In addition, the solution becomes increasingly turbid, an indication for micelle formation in THP where 4-PVP is insoluble. The reaction mixture is allowed to heat up to −20 °C, and the reaction is terminated with methanol.

The resulting polymers are precipitated in low-boiling petroleum ether and dried in vacuo at 50 °C for 2 days. As seen by a complete yield, the added 4-PVP can be regarded as fully polymerized. Therefore, micelle formation seems not to affect further polymerization.

(II.2) Polymer Characterization. GPC measurements on the block copolymers are performed in THF (60.0 °C) and DMF (70.0 °C) with a column combination 10^6–10^4–10^3 Å from PSS Co. The signals are detected with a two-detector combination (UV detector, Spectra Physics 100; RI detector, Shodex RI 61) which allows for the direct determination of molecular weight and the estimation of the relative composition. In addition, the relative composition of the block copolymers is controlled by ^{1}H-NMR and elementary analysis.

(II.3) Static and Dynamic Light Scattering. Light scattering experiments were carried out in toluene, tetrahydrofuran, butyl acetate, and butanone at 20.0 °C. The spectrometer and procedure for simultaneous static and dynamic light scattering are extensively described in previous publications.[14,15] The measurements are performed at the 647.1-nm line of a krypton ion laser (Spectra Physics 2025). We adopt for the refractive index increment the values for polystyrene, since PS and 4-PVP are nearly isorefractive.

The solutions are purified by 10-fold filtering through Millipore 0.45-μm PTFE filters. Usually, no significant loss of concentration due to filtering can be detected. The final concentrations range between 10^0 and 10^{-2} g/L.

(III) Results and Discussion

(III.1) Synthesis and GPC Results. The characterization of the polystyrene precursors and the corresponding blocks by GPC is summarized in Table 1.

We observe that the polystyrene parts of the block copolymers are quite narrowly distributed. The complete blocks become broader which is possibly due to a more heterogeneous chain growth within the micelles which

® Abstract published in *Advance ACS Abstracts*, May 1, 1994.

0024-9297/94/2227-3276$04.50/0

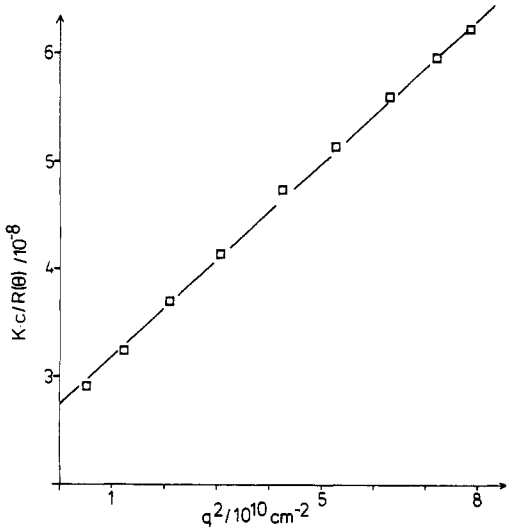

Figure 1. Angular dependence of the renormalized light scattering intensity in a Zimm presentation. The experiment is performed with AS7 in toluene at c = 0.1 g/L.

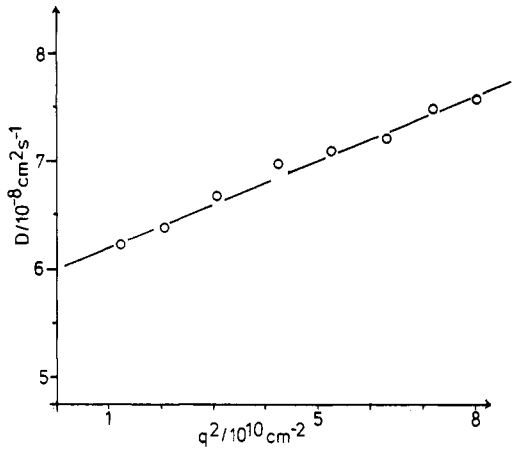

Figure 2. Angular dependence of the apparent diffusion coefficient D of AS7 in toluene at c = 0.1 g/L.

Table 1. GPC Data of Styrene/4-Vinylpyridine Block Copolymers and the Corresponding Polystyrene Precursors

	PS			PS/4-PVP			
sample	M_w	M_n	U	M_w	M_n	U	X_{VP}
AS3	97 200	91 700	1.06	120 000	112 000	1.07	0.19
AS7	30 000	27 300	1.10	45 000	40 200	1.12	0.33
AS13	81 200	79 400	1.02	116 000	112 000	1.03	0.30
AS14	36 600	32 400	1.13	43 600	38 200	1.14	0.16

already form during polymerization. In all cases, only traces of pure polystyrene are detected, indicating a nearly complete cross-step from styrene to 4-vinylpyridine.

Table 1 also includes the data for the relative composition as obtained by ^{1}H-NMR and elementary analysis.

(III.2) Static and Dynamic Light Scattering. Static and dynamic light scattering on these block copolymers reveals a quite complex behavior in dilute solution which depends on the solvent used. In toluene and butanone, the data can be evaluated by standard procedures; the typical procedure of data evaluation is exemplarily delineated in detail for the sample AS7 in toluene.

Figures 1 and 2 present the q-dependence of the static intensity and the apparent diffusion coefficient D_{app}, respectively. From the intercept of Figure 1, we can calculate a molecular weight of 36.1 × 10^6, corresponding to an aggregation number of 800 block copolymers per micelle. This number, within experimental error, appears to be independent of concentration, and even at concentrations as small as 10^{-5} g/cm^3, no indications of a critical micelle concentration (cmc) are observed. Considering the large radius of gyration $r_G \equiv \langle s^2 \rangle_z^{0.5}$ of about 70 nm, it is relevant that the static data are best linearized by the Zimm plot. This fact can be related to a nonspherical structure.

In all cases, the time correlation functions of dynamic light scattering can almost be described by a single-exponential relaxation; a cumulant analysis of the relaxation function reveals values for the second cumulant between $0.02 \leq u_2 \leq 0.10$. It is possible to relate these values to micelle polydispersities;[16] by assuming a logarithmic normal distribution, we obtain micelle polydispersities between $M_W/M_n \approx 1.1$ ($u_2 = 0.02$) and 1.5 ($u_2 = 0.10$).

In the present case of moderate polydispersities and small concentrations, the angular dependence of D_{app} can be linearized using eq 1. By insertion of the thermodynamic

$$D_{app} = D_0(1 + Cq^2 r_G^2) \tag{1}$$

diffusion coefficient D_0 in the Stokes–Einstein equation, we calculate a hydrodynamic radius of r_H = 63.8 nm for AS7 micelles in toluene.

Assuming nondrained hydrodynamic behavior, an average polymer density Φ within the micelle can be calculated from r_H and M according to eq 2. For AS7 in toluene, we

$$\Phi = \frac{3M}{4\pi r_H^3 N_L} \tag{2}$$

obtain Φ = 0.055, a surprisingly low value.

The ratio $P \equiv r_G/r_H$ is a sensitive fingerprint of the inner density profile. A value of P = 1.1 exceeds the values for spherical structures, $P \leq 0.775$. (For a more detailed discussion of this limit, see ref 17.) For cylinders with length L and diameter d, eq 3 holds.[18]

$$r_G/r_H(\text{cyl}) = \frac{1}{\sqrt{3}}(\ln(L/d) + 0.38) \tag{3}$$

From P = 1.1, we calculate $L/R \approx 4.6$. It must also be considered that P values larger than 1 cannot be related solely to a cylindrical shape but to all geometries with different axial ratios. First experiments with electron microscopy, however, support the structure model of short, slightly bent cylinders. These data and analogous experiments on metalated micelles will be presented in a forthcoming publication.[19]

In the absence of long-time intramolecular relaxations, the normalized slope C (see eq 1) of the angular dependence of dynamic light scattering is also related to the shape of the micelle. The value of AS7 in toluene, C = 0.07, is smaller than the theoretical value for a Gaussian chain ($C \approx 0.16$) but is typical for rodlike or ellipsoidal structures.[20]

The same data analysis is performed for four block copolymer samples selected from a wider set of samples where the typical phenomena are most pronounced. Table 2 summarizes these data. When the data evaluation is disturbed by intermolecular effects, only very low concentrations are considered.

We have chosen four different solvents with different solvent parameter δ (butyl acetate δ = 8.5; toluene δ = 8.9; THF δ 9.1; butanone δ = 9.3, taken from ref 9) covering nearly the complete range of moderate or good solvents for polystyrene). Solvents with remarkably higher polarities (as DMF) were excluded since they dissolve the poly(vinylpyridine) block too.

Table 2. Polymer Analytical Data of Four Different PS-*b*-4-PVP Copolymers in Four Different Solvents[a]

sample	solvent	$M_w/10^6$	Z	r_G/nm	r_H/nm	r_G/r_H	Φ_H
AS3	butyl acetate	27.5	229	45.2	57.3	0.789	0.058
$M_w = 1.2 \times 10^5$	toluene	19.2	160	43.4	69.7	0.623	0.022
$X_{VP} = 0.19$	THF	7.8	65	34.2	53.4	0.640	0.020
	butanone	13.9	116	37.7	49.3	0.764	0.026
AS7	butyl acetate	37.2	827	53.4	51.8	1.031	0.106
$M_w = 4.5 \times 10^4$	toluene	36.1	802	70.2	63.8	1.100	0.055
$X_{VP} = 0.33$	THF	1.81	40	21.9	28.8	0.759	0.030
	butanone	2.9	65	21.5	24.3	0.885	0.080
AS13	butyl acetate[b]	58.0	500	113.5	86.8	1.304	0.035
$M_w = 1.16 \times 10^5$	toluene[b]	35.0	302	64.2	75.1	0.885	0.033
$X_{VP} = 0.30$	THF	18.5	159	45.5	74.4	0.612	0.018
	butanone	26.1	230	68.5	81.3	0.842	0.037
AS14	butyl acetate[c]	4.5	122	24.2	29.7	0.815	0.068
$M_w = 4.36 \times 10^4$	toluene	5.1	138	25.9	34.5	0.751	0.049
$X_{VP} = 0.16$	THF[d]	0.84	23	48.6	59.7	0.814	0.002
	butanone[d]	0.92	25	40.6	44.0	0.922	0.004

[a] Presented are the molecular weight M_w, the aggregation number Z, the radius of gyration r_G, and the hydrodynamic radius r_H. The characteristic ratio r_G/r_H is related to the structure. Φ_H is the calculated volume fraction of polymer inside a hydrodynamically equivalent sphere of r_H. The data are usually determined from concentrations between 10^{-2} and 10^0 g/L. [b] Ultrasonification is needed for a complete micellar dissociation of the samples. Without ultrasonification, micelle/micelle aggregates of larger size and polydispersity dominate the scattering behavior. [c] The measurement is strongly disturbed by intermolecular structure formation. The data are afflicted with comparably high errors. [d] At low concentrations, a drop of the scattering intensity is observed. The molecular parameters of the micelles are taken from 0.2 to 1 g/L.

Sample AS3 produces spherical micelles in all solvents as proven by the P value. In THF and toluene, P is consistently lower than the hard-sphere value of 0.775. Such low P values cannot be explained theoretically but are frequently observed for soft-spherical structures.[17] A spherical structure of the micelles is expected for copolymers with the relative low 4-VP content of 19%.

We expect that the aggregation number depends on the solvent quality for both blocks. In other words, the micelle size is controlled by the tendency toward separation to a nonsoluble micelle core as well as by the osmotic repulsion of the solvating chains. In the strong segregation limit, the first contribution can be expressed by an interfacial energy between the micelle core and the solvent which can be related to the difference of the δ values of the solvent and 4-PVP.

In the present data set, it is obvious that the aggregation number decreases with increasing "solvent" quality for 4-PVP (butanone > THF > toluene > butyl acetate). The influence of the solvent quality for PS (toluene > THF > butanone > butyl acetate) is hardly seen in the data; one might speculate that the lower Z in THF compared to butanone might be due to polystyrene repulsion.

Similar trends are seen for sample AS14 which exhibits a similar composition but only a third of the chain length. The absolute length of the 4-PVP block (ca. 70 units) is in a range where the copolymers become slightly soluble: at low concentrations, we observe in THF and butanone a critical micelle concentration as indicated by a strong drop of the static light scattering intensity at low concentrations.

The existence of a cmc for these systems is accompanied by a quite low aggregation number and very low Φ values. As taken from higher concentrations (0.2–1 g/L), the hydrodynamic radius is already about 50% of the contour length of the chains. One might conclude that these micelles are more like concentration fluctuations, transient structures in a fast dynamic exchange, but not spherical micelles with a solid- or gellike core.

The micelle architecture of AS7 is more complex: the micelles in toluene are anisometric, probably short cylinders, as seen by a P value being bigger than 1. This structure assumption would fit with the relative 4-VP content of 33% where a cylindrical morphology is observed in the bulk. In THF and in butanone which are more polar, AS7 micelles with spherical shape are obtained. The anisometry or the large P value is followed by an aggregation number being much larger (400–800 block copolymer per micelle) than observed in the case of spherical micelles (60–200 in the stable systems). For sterical reasons, this underlines the assumption of a cylindrical or cigar-type geometry.

It is interesting to follow these trends in the case of AS13, which again has about the same composition as AS7 but a 3 times larger chain length. Here, cigar-type micelles (high P value, high Z) are only observed in the case of the worst solvent for 4-PVP, butyl acetate, whereas all other solvents produce spherical morphologies. The direct comparison of AS7 and AS13 shows the influence of the solvating chains on the micelle morphology: the osmotic repulsion of the solvating chains which depends on the absolute molecular weight of the solvating blocks tends toward a maximum accessible volume which is realized in the spherical morphology. Consequently, anisometric micelles can only be observed in the case of small polymer chains or under bad solvent conditions for the solvating chain. As seen in the solvent variation, very bad solvent conditions and related high interfacial energies for the inner blocks are also needed for the formation of an extended micellar shape.

It is interesting to note that a very similar, anisometric micelle morphology is already referred to in the literature for a PS/PMMA block copolymer with a relative PS content of about 38%.[2] Here, the micelles are best described by prolate ellipsoids with an axial ratio of $f \approx 4$.[2]

The spherical micelles are generally quite monodisperse, whereas the polydispersity is increased for the nonspherical micelles. Appparently, the energy control of the size is less pronounced for cylinders which is reasonable and also known for low molecular weight surfactants.

In the present experiments, the limit of the aggregation number for spherical micelles is about 200 which represents already a strong geometrical confinement for the block copolymer chains.

Taking, for instance, AS3 in toluene and assuming for simplification no overlapping of neighboring block copolymers, we may calculate the cone in which each polymer is located. Under the assumption that each chain extends from the center of the micelle (one end located in the core)

to the surface of the micelle, the height of the cone can be assigned to r_H of the micelle (ca. 70 nm). The basis of the cone or the averaged distance between the chains in the outer region of the micelle is calculated from the size and Z and is obtained as about 20 nm. Although calculations regarding the chain behavior close to the core have to await the core structure characterization by SANS, we can roughly estimate a core/shell interface for AS3 of $(3.2\ \text{nm})^2$.

It is now interesting to relate these geometric values with characteristics of the hypothetically isolated block copolymer molecule of a polystyrene chain of the same molecular weight. For AS3 in toluene, we can estimate an "unperturbed" end-to-end distance of 34 nm,[21] compared to $r_H \approx 70$ nm in the micellar geometry. Therefore, the incorporated polystyrene chains can be regarded as remarkably stretched, which is due to the osmotic force directing to the outside of the micelle. However, the area per chain on the outside of the micelle perpendicular to the chain stretching is still on the order of r_G^2. This combination also results in lower polymer densities, as seen by the comparably small Φ values inside the micelles. Although block copolymer micelles, as the analogous many-arm stars, are regarded to be quite compact, they exhibit lower densities than a hypothetically isolated block copolymer chain.

AS13 (chain length comparable to AS3) is producing in toluene spherical micelles with still larger aggregation numbers. As a result, r_H and the related chain stretching is another 10% larger. The corresponding micelle surface area per chain, however, is $(17.4\ \text{nm})^2$ and the core/shell interface area per chain $(3.3\ \text{nm})^2$. Apparently, the higher aggregation number mainly results in a higher chain stretching; the chain–chain distance in the micellar geometry in the tangential direction is just slightly affected. This effect underlines the importance of the osmotic chain/chain repulsion of the solvating chains for the control of the micelle architecture. Similar trends are seen for the other solvents.

This expansion of the chains in block copolymer micelles is expected by theory[22-24] and already described in some experiments (e.g., refs 25 and 26). In strick analogy to the data treatment of Gast et al.,[25] we can use the string-of-blob model of Witten et al.[22] to describe the chain expansion in a starlike environment.

Taking again AS3 in toluene as an example, we calculate with the known constants for polystyrene a micellar r_H of about 63.5 nm, compared to the experimental value of 70 nm. This difference, a slight underestimation, is not too bad, especially in spite of the fact that this theory does not consider expelling interface effects between core and corona chains.

For AS7 micelles and their still higher geometrical confinements, similar calculations for the chain geometry are complex since these micelles do not exhibit spherical symmetry. We can only compare the contour length of the primary block copolymer ($L \approx 108$ nm) or its radius of gyration in toluene ($r_G \approx 7.7$ nm) with the observed micelle radius of gyration of about 70 nm which again underlines the anisometric nature of these micelles. In this case, the estimate of the chain stretching requires a more precise determination of the axial ratio.

(III.3) Description of the Aggregation Behavior. In THF as well as in butanone, all four block copolymers form micelles with spherical morphology. In these cases, we are able to test theoretical predictions for the block copolymer aggregation in selective solvents.

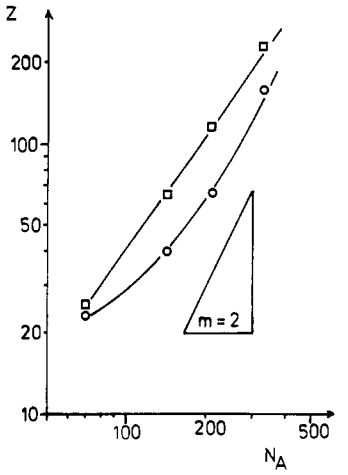

Figure 3. Aggregation number Z depending on the length of the 4-VP block, N_A. Measurements (□) in butanone and (○) in THF.

In his pioneering work,[27] de Gennes proposed that the aggregation number Z only depends on the number of monomers in the associating block, N_A, as:

$$Z \sim N_A \quad \text{when the interface energy is large} \tag{4a}$$

$$Z \sim N_A^{0.5} \quad \text{when the interface energy is low} \tag{4b}$$

A more recent theory by Leibler et al.[28] for block copolymers mixed with homopolymers gave a different result:

$$Z \sim N_A^{0.6} \tag{5}$$

In both treatments, the solvating block is considered to have no influence on the micelle architecture.

Nagarajan amd Ganesh numerically solved an expression for the free energy of block copolymer micelles which treats block copolymers analogous to low molecular weight surfactants.[29] For a system in the strong segregation limit, they obtained:

$$Z \sim N_A^{1.1} N_B^{-0.2} \tag{6}$$

In this theory, both scaling exponents depend on solvent quality for both blocks.

Figure 3 shows our data for the block copolymers in THF (lower curve) and butanone (upper curve) depending on the length of the 4-VP block N_A. Clearly, the dependence of Z is stronger than the predicted ones. Pushing a scaling relation through the data point results in an exponent being between 1.5 and 2. It must be underlined that a similar behavior was detected by Tuzar and Munk where exponents between 1.6 and 1.9 were obtained.[37]

An exponent of 2 is also derived from simple space-filling calculations, analogous to treatments known for the micellization of low molecular weight surfactants.

The argumentation starts from the observation that the two relevant energy contributions, the interface energy between core and solvent and the osmotic force of the micelle-forming chains, balance in a way that a constant interface area per chain, b^2, is stabilized:

$$4\pi(R_c^2/Z) = b^2 \tag{7}$$

This is in contrast to all current theoretical approaches on block copolymer micelles but in good agreement with the observations of Munk and Tuzar.[37] It must be stressed

that all energy considerations or interaction parameters of polymers A and B and solvent enter the description only via b^2.

Assuming that the micelle core is strongly segregated and behaves like a gellike polymer droplet with a swelling ratio Q, we write for the volume of one A chain inside the core:

$$(4/3)\pi(R_c^3/Z) = N_A a^3 Q \tag{8}$$

with a^3 being the monomer volume (mole volume of monomer units divided by Avogadro's number) and R_c the radius of the core.

Having these constraints for surface and volume, we obtain:

$$Z = 36\pi N_A^2 (a^6/b^6) Q^2 \tag{9}$$

$$R_c = 3N_A Q(a^3/b^2) \tag{10}$$

The resulting N_A^2 law of eq 9 is in fact quite close to our experimental data as predicted in Figure 3.

It is also interesting to note that the strong dependence of Z and R_c on N_A inherently produces two criteria of micelle destabilization and a resulting shape transition.

(a) The core radius increases with an exponent of N_A significantly larger than 0.5 (in the simple description linearly with N_A). At high Z, i.e., core radii in the region of the end-to-end distance of the 4-PVP block, this results in an effective stretching of the inner chains which destailizes the spherical shape.

(b) According to the Witten description[22] the increase of N_A via the aggregation number results in a strong increase of chain stretching of the corona chains. Also this entropy loss can induce a sphere-to-rod transition.

Within the presented data set, it is not straightforward which contribution is dominant under the applied good solvent conditions.

The comparison of the data of samples AS7 and AS13 in toluene shows that the second contribution may be more important: although AS13 has a higher N_A, it still exhibits spherical morphology since its longer polystyrene block is more easily stretched.

A direct comparison of the core radius (calculated for a solid core) with the end-to-end distance of the A block, however, indicates that prolate micelles are formed when R_c exceeds the Gaussian dimensions of the chain. This occurrence is probably accidental, and a wider data set is needed to mark the right criterium for the shape transition.

(III.4) Order Formation in Dilute Solution. In this chapter, we want to stress one phenomenon which is observed—more or less pronounced—in most of our block copolymer solutions: the effect of a long-range order formation. This phenomenon is observed as a pronounced decrease of static light scattering at small angles when the concentration is properly chosen. A typical set of data is presented in Figure 4 which shows AS7 in butyl acetate at a concentration of c = 1 g/L. We observe that the form factor of the individual micelles which dominates the angular dependence at high q values is superimposed by an intermolecular interference factor, resulting in a strong decrease of the light intensity at low q's. This behavior is paralleled by a similar dependence of $D_{app}(q)$ which shows an anomalous increase at the same critical $q \approx 1.3 \times 10^5$ cm^{-1}. Taking the molecular weight of the micelles determined at very low concentrations as constant, we can calculate from the concentration a maximal particle distance of 460 nm, which is about the Bragg spacing

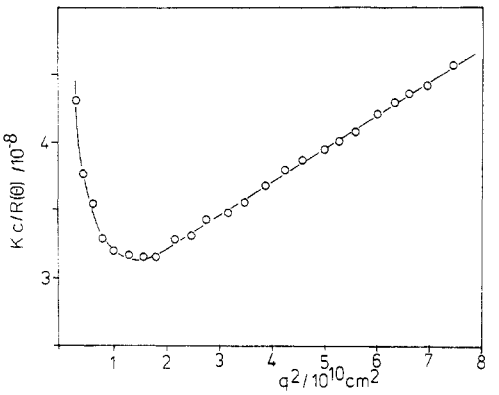

Figure 4. Angular dependence of the renormalized static light scattering intensity of sample AS7 in butyl acetate at c = 1 g/L. The line just guides the eye.

Table 3. Viscosity Data of Styrene/4-Vinylpyridine Block Copolymers[a]

	THF		toluene	
sample	$[\eta]$/(cm^3 g^{-1})	Φ_{vis}/(g/cm^3)	$[\eta]$/(cm^3 g^{-1})	Φ_{vis}/(g/cm^3)
AS3	46.4	0.054	42.5	0.058
AS7	17.5	0.143	16.2	0.154
AS13	40.3	0.062	38.6	0.065
AS14	23.8	0.105	21.2	0.118

[a] $[\eta]$ is the intrinsic viscosity and Φ_{vis} the volume fraction of polymer inside r_η, as calculated from the Einstein law.

related to the observed scattering peak. Such a behavior indicates a strong repulsion of the micelles with an intermolecular potential being effective in the few hundred nanometer range.

A similar structure formation is already described in the literature, for instance, for block copolymers consisting of PS and PMMA blocks[2,30] or even pure 4-PVP in nitromethane.[31] Such long-range interactions (interaction length being 3–5 times the micelle diameter) are most probably of the Coulomb type, although the presented data originate from nonionic polymers in nonionic organic solvents. For such a system, the self-charging frequently seen in aqueous colloidal systems is generally not observed.

However, Chu et al. experimentally proved that polydiacetylenes in nonaqueous solvents spontaneously charge up[32] when the solvent quality is poor and aggregation occurs. The formation of charges is attributed to the different polarizability of colloidal particles and solvent or to the so-called Coehn's law.[33] On the contrary to the diacetylenes, the occurrence of the present structure peak cannot be related to the dielectric constant of the solvents. More likely, the structure peak occurs in solvents which may contain some spurious amounts of water or ionic impurities. A more detailed analysis of this phenomenon is currently in progress including conductivity measurements and determination of the electrophoretic mobility by capillary electrophoresis.

(III.5) Viscometry of Block Copolymers. Another standard technique for the characterization of polymer hydrodynamics is viscometry. The related quantity, the intrinsic viscosity $[\eta]$, is a measure of the inverse polymer density inside a hydrodynamically equivalent sphere.[34] Some exemplary data for our block copolymers are listed in Table 3.

The comparison of the volume fractions of polymer within the hydrodynamic effective radius r_η as calculated from viscometry with the corresponding volume fractions of Table 2 as calculated from r_H and M_W discloses large deviations, although it is known that these values should be very similar for polymer systems with spherical

symmetry[35] and differ only by 30% in the case of linear polymer chains.[36]

On the other hand, the intrinsic viscosities determined for micelles are just slightly smaller than linear polystyrene chains of the same molecular weight as the parental block copolymers.[9]

Obviously, the micelles deaggregate during shear. This conclusion is supported by two additional observations:

(i) We never observed micelle formation in our MALLS detector of the GPC setup where light scattering is performed in a capillary shear field.

(ii) Under appropriate conditions, the turbidity of a block copolymer solution vanishes during fast stirring.

A variation of the applied shear rate by a factor of 10 ($10\,000 < \gamma < 1000\ s^{-1}$) by the capillary size only alters the intrinsic viscosities of the micelles by less than 10%. It means that the critical shear rate is very small, or, in other words, the longest relaxation time of the micelles is comparably long (longer than 1 ms). It must be underlined that this phenomenon is not considered in some experimental papers where viscometry was applied for the characterization of micellar properties. The phenomenon of shear deaggregation has also some implications for the coverage of planar surfaces by block copolymers which can be supported by shear.

(IV) Conclusion and Outlook

We have shown that the micelle size and structure of PS/4-PVP block copolymer micelles can be adjusted via the related composition, chain length, and solvent quality.

From our data and referred experiments described in the literature, some general trends can be extracted:

(1) Spherical block copolymer micelles consist of 20–500 block copolymers. The aggregation number essentially follows the length of the nonsoluble block A *and* the difference in the δ parameter between solvent and block A, as reflected in the interface energy.

(2) A second structure-relevant but weaker energy contribution results from the osmotic chain–chain repulsion of the solvating blocks: the better the solvent quality for the outer block, the smaller the micelles are.

(3) A part of the osmotic repulsion is compensated via a stretching of the solvating chains. This stretching can be described by the Witten model which slightly underestimates the elongation of chains.

(4) The stretching of the corona chains results in a destabilization of the spherical shape. Anisometric micelles are formed when a critical energy loss is exceeded. These micelles are characterized by high aggregation numbers (500–800) and a prolate shape.

Obviously, also a number of new questions arise. On the one hand, a more precise characterization of the micelle core with SANS is necessary for a better description of the micelle architecture. On the other, the question of the scaling relation of the aggregation number on both block lengths has to be experimentally answered on a broader sample base. Finally, the physical origin of the observed ordering phenomenon is still unknown and needs experimental clearance.

Acknowledgment. Financial support by the Deutsche Forschungsgemeinschaft, the Fonds der Chemischen Industrie, and the Marburger Zentrum für Materialwissenschaften is gratefully acknowledged.

References and Notes

(1) Krause, S. *J. Phys. Chem.* **1964**, *68*, 1948.
(2) Utiyama, H.; Takenaka, K.; Mizumori, M.; Fukuda, M.; Tsunashima, Y.; Kurata, M. *Macromolecules* **1974**, *7*, 515.
(3) Tuzar, Z.; Kratochvil, P. *Adv. Colloid Interface Sci.* **1976**, *6*, 201.
(4) Riess, G.; Bahadur, B.; Hurtrez, G. In *Encyclopedia of Polymer Science & Engineering*; Wiley: New York, 1985; p 324.
(5) Kotako, T.; Tanaka, M.; Hattori, M.; Inagaki, H. *Macromolecules* **1978**, *11*, 138.
(6) Tuzar, Z.; Plesti, J.; Konak, C.; Hlavata, D.; Sikora, A. *Makromol. Chem.* **1983**, *184*, 2111.
(7) Cogan, K. A.; Gast, A. P. *Macromolecules* **1990**, *23*, 745.
(8) Vagberg, L. J. M.; Cogan, K. A. M.; Gast, A. P. *Macromolecules* **1991**, *24*, 1670.
(9) Brandrup, J., Immergut, E. H., Eds. *Polymer Handbook*; Wiley: New York, 1974.
(10) Grosius, P.; Gallot, Y.; Skoulios, A. *Makromol. Chem.* **1970**, *132*, 35.
(11) Ishizu, K.; Kashi, Y.; Fukutomi, T.; Kakurai, T. *Makromol. Chem.* **1982**, *183*, 3099.
(12) Antonietti, M.; Fölsch, K. J. *Makromol. Chem., Rapid Commun.* **1988**, *9*, 423.
(13) Antonietti, M.; Ehlich, D.; Fölsch, K. J.; Sillescu, H.; Schmidt, M.; Lindner, P. *Macromolecules* **1989**, *22*, 2802.
(14) Bantle, S.; Schmidt, M.; Burchard, W. *Macromolecules* **1982**, *15*, 1604.
(15) Antonietti, M.; Schmidt, M.; Schuch, H.; Sillescu, H. *Macromolecules* **1988**, *22*, 736.
(16) King, T. A.; Treadaway, M. F. *J. Chem. Soc., Faraday Trans. 2* **1977**, *73*, 1616.
(17) Antonietti, M.; Bremser, W.; Schmidt, M. *Macromolecules* **1990**, *23*, 3796.
(18) Broersma, S. J. *J. Chem. Phys.* **1960**, *32*, 1626.
(19) Antonietti, M.; Heinz, S., to be published.
(20) Schmidt, M.; Stockmayer, H. *Macromolecules* **1984**, *17*, 509.
(21) Burchard, W.; Schmidt, M. *Macromolecules* **1981**, *14*, 210.
(22) Grest, G. S.; Kremer, K.; Witten, T. A. *Macromolecules* **1987**, *20*, 1376.
(23) Milner, S. T. *Science* **1991**, *252*, 905.
(24) Dan, N.; Tirrell, M. *Macromolecules* **1992**, *25*, 2890.
(25) Coogan, K. A.; Gast, A. P.; Capel, M. *Macromolecules* **1991**, *24*, 6512.
(26) Balsara, N. P.; Tirrell, M.; Lodge, T. P. *Macromolecules* **1991**, *24*, 1975.
(27) de Gennes, P.-G. In *Solid State Physics*; Liebert, J., Ed.; Academic: New York, 1978; supplement 14, p 1.
(28) Leibler, L.; Orland, H.; Wheeler, J. C. *J. Chem. Phys.* **1983**, *79*, 3550.
(29) Nagarajan, N.; Ganesh, K. *J. Chem. Phys.* **1989**, *90*, 5845.
(30) Utiyama, H.; Takenaka, K.; Mizumori, M.; Fukuda, M. *Macromolecules* **1974**, *7*, 28.
(31) Seely, G. R. *J. Phys. Chem.* **1967**, *71*, 2091.
(32) Xu, R.; Chu, B. *Macromolecules* **1989**, *23*, 4523.
(33) Coehn, A.; Raydt, V. *Ann. Phys.* **1909**, *30*, 777.
(34) $[\eta] = 2.5/\Phi$, where Φ is the volume fraction of polymer inside a hydrodynamically equivalent sphere.
(35) Antonietti, M.; Bremser, W.; Schmidt, M. *Macromolecules* **1990**, *23*, 3796.
(36) McDonnell, M. E.; Jamieson, A. M. *J. Macromol. Sci.* **1977**, *B13*, 67.
(37) Qin, A.; Tian, M.; Ramireddy, C.; Webber, S.; Munk, P.; Tuzar, Z. *Macromolecules* **1994**, *27*, 120.